



ChemComm

**Water-Mediated Polyol Synthesis of Pencil-like Sharp Silver Nanowires Suitable for Nonlinear Plasmonics**

Journal:	<i>ChemComm</i>
Manuscript ID	CC-COM-06-2019-004743.R1
Article Type:	Communication

SCHOLARONE™  
Manuscripts



Journal Name

COMMUNICATION

## Water-Mediated Polyol Synthesis of Pencil-like Sharp Silver Nanowires Suitable for Nonlinear Plasmonics

Received 00th January 20xx,  
Accepted 00th January 20xx

Tomoko Inose,<sup>a</sup> Shuichi Toyouchi,<sup>b</sup> Gang Lu,<sup>c</sup> Kazuki Umemoto,<sup>d</sup> Yuki Tezuka,<sup>d</sup> Bozhang Lyu,<sup>d</sup> Akito Masuhara,<sup>d</sup> Eduard Fron,<sup>b</sup> Yasuhiko Fujita,<sup>b,e</sup> Kenji Hirai,<sup>a</sup> Hiroshi Uji-i<sup>\*a,b</sup>

DOI: 10.1039/x0xx00000x

www.rsc.org/

**We report a simple method to control end shape of silver nanowires by adding pure water in the conventional polyol synthesis. Use of 0.2 – 0.4 % (v/v) water in ethylene glycol as a solvent provides pencil-like silver nanowires with sharp-end in high yield. We have demonstrated remote excitation of SHG on the sharp nanowires, promising a point light source for super resolution microscopy.**

Silver nanowires (AgNWs) are one of the most interesting and useful metal nanostructures due to their unique electronic, thermal, and optical properties. The development of the synthesis has been incentivized by their potential applications, including plasmonic waveguide remote sensing<sup>1-3</sup> and super resolution/highly sensitive micro/spectroscopy, such as atomic force microscopy,<sup>4</sup> tip-enhanced Raman scattering,<sup>5,6</sup> and surface enhanced Raman scattering in a single live cell.<sup>7</sup> Fiévet *et al.* pioneered polyol synthesis as an easy and simple method to produce colloidal gold/silver nanoparticles.<sup>8-11</sup> The synthesis hinges on the reduction of an inorganic salt by a polyol, e.g. ethylene glycol (EG), at an elevated temperature. This method has been widely recognized after Xia's group reported a condition to produce AgNWs with high aspect ratio in the presence of polyvinylpyrrolidone (PVP) as a capping agent.<sup>12-15</sup>

So far, several researchers have focused on various parameters on the AgNWs synthesis to improve the process in terms of yield and/or control of diameter/length of the final products. This ranges from reaction temperature,<sup>16, 17</sup> molecular weight of capping reagents,<sup>12</sup> injection rate of AgNO<sub>3</sub><sup>17</sup> to concentration of PVP and AgNO<sub>3</sub>.<sup>16,17</sup> Moreover, a

few groups have recently engineered the end morphology.<sup>4, 18, 19</sup> For example, Liu *et al.* used (NH<sub>4</sub>)<sub>2</sub>CO<sub>3</sub> as an additive, in which both NH<sub>4</sub><sup>+</sup> and CO<sub>3</sub><sup>-</sup> effectively reduced the amount of Ag<sup>+</sup> in the growth solution. This effectively accelerates the oxidative etching, resulting in sharpening NW end.<sup>4</sup>

In addition to the aforementioned applications, nonlinear optical effects (NLO) of metal nanostructures accompanied with excitation of surface plasmon polaritons (SPPs), e.g. second harmonic generation (SHG)<sup>20, 21</sup> and/or wave-mixing,<sup>22, 23</sup> called nonlinear plasmonics, have been recently attracting researchers because of the high sensitivity, ultrafast response, and possibility to scale down nonlinear optics into nanometre scale.<sup>24</sup> AgNWs are one of the most promising candidates for NLO applications due to their excellent plasmonic waveguiding properties<sup>25</sup> that could provide a unique point light source at nanoscale for super-resolution microscopy.<sup>26</sup> For such applications, the end morphology plays a crucial role, because light-coupling in/out as well as NLOs occur at their ends. Thus, further development of end morphology control is required.

In this paper, we report an active engineering of AgNWs' end morphology in order to enhance and control NLO response. We show that the presence of trace amount of water in the polyol reaction dramatically affects on the end morphology. We investigated various reaction conditions, including amount of water to be added, reaction time, and timing of water injection. While trapezoid-like end shape is often obtained in the typical polyol synthesis, sharp-end morphology can be produced in the presence of appropriate amount of water in EG in the yield over 90%. We finally demonstrate highly consistent, enhanced NLO responses on sharp-end AgNWs owing to tight confinement of SPPs at the end, promising for nonlinear plasmonic waveguiding and a point light source for super resolution microscopy.

First, we performed a standard polyol synthesis of AgNWs. Briefly, AgNO<sub>3</sub> EG solution was added drop-wise at an injection rate of 100 μL/min into a pre-refluxed EG solution of PVP in the presence of CuCl<sub>2</sub> at 160 °C. The reaction solution was further kept at 160 °C for 1 hour after injecting all the AgNO<sub>3</sub> solution (see the detail in ESI). We obtained AgNWs with a

<sup>a</sup> Research Institute for Electronic Science (RIES), Hokkaido University, N20W10, Sapporo 001-0020.

<sup>b</sup> KU Leuven, Departement Chemie, Celestijnenlaan 200F, 3001 Heverlee, Belgium.

<sup>c</sup> Nanjing Tech University, Institute of Advanced Materials & Key Laboratory of Flexible Electronics (KLOFE), Jiangsu National Synergistic Innovation Center for Advanced Materials (SICAM), 30 South Puzhu Road, Nanjing 211816, Jiangsu, People's Republic of China

<sup>d</sup> Graduate School of Science and Engineering, Yamagata University, Yonezawa, Yamagata 992-8510, Japan.

<sup>e</sup> Toray Research Center, Inc., Sonoyama 3-3-7, Otsu, 520-8567 Shiga, Japan.

† Electronic Supplementary Information (ESI) available: See DOI: 10.1039/x0xx00000x

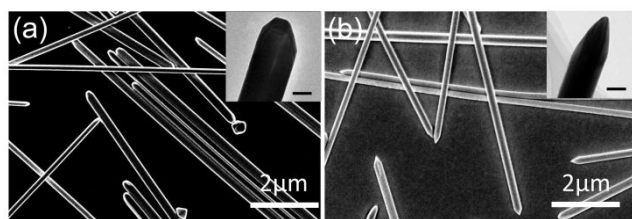
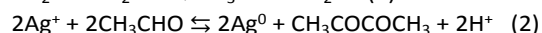
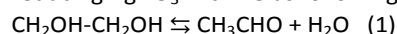


Fig. 1 SEM images of AgNWs synthesized in pure EG (a) and in EG containing 0.2% (v/v) of H<sub>2</sub>O (b). The insets are TEM images of nanowire end (Scale bar in the insets 50 nm).

typical length of 10 to 50  $\mu\text{m}$  and averaged diameter of  $200 \pm 48$  nm (Fig. 1a). The proposed mechanism to explain the AgNWs growth from nuclei is Ostwald ripening. Through this mechanism, Ag nanoparticles with larger sizes are able to grow by expensing smaller ones. A capping agent of PVP adsorbs preferentially on the {100} side surfaces rather than on the {111} ends, thus inhibits the lateral growth and induces preferential longitudinal growth of {111} facets.<sup>13</sup> Following this mechanism, crystal structure at the middle of AgNWs is thus always the pentagonal dipyramid. Under this conventional synthesis condition, we found that nearly 100 % of nanowires had trapezoid-like end morphology, where {111}, {220}, {311} and {331} coexist at the end (Fig. S1).

In the second synthesis, a small amount of Milli-Q water was mixed with EG in advance, and this mixed solvent was used for all the precursor solutions. Except for adding water, the synthesis protocol was identical to the first synthesis. As seen in the SEM image of AgNWs synthesized in the presence of 0.2 % (v/v) water (Fig. 1b), most of AgNWs possess very sharp end morphology. We estimated to be more than 90 % of AgNWs with sharp-end and less than 10 % with trapezoid-like morphology. The facet of the sharp-end consists of many facet, i.e. {111}, {200}, {220}, and {311} (Fig. S2). The radius of curvature of the sharp AgNWs synthesized in the presence of 0.2 ~ 0.4 % (v/v) water is estimated to be  $27 \pm 5$  nm, while that of trapezoid AgNWs is typically  $64 \pm 10$  nm.

In a typical polyol synthesis, AgNWs are obtained by reducing AgNO<sub>3</sub> with EG as following two reactions.<sup>8</sup>



At the beginning of the reaction, concentration of Ag<sup>+</sup> is very high and the limiting parameter for reduction is the concentration of acetaldehyde. When extra water is added in the reaction, the equilibrium in equation (1) should be shifted to the left, resulting in lower amount of acetaldehyde. Reduction rate of Ag<sup>+</sup> to Ag<sup>0</sup> is thus decelerated. Indeed, according to inductively coupled plasma optical emission spectroscopy (ICP-OES) analysis, less reduction occurs at higher amount of water; at the very beginning of the reaction, 91.6 % and 87.9% of Ag<sup>+</sup> were reduced to Ag<sup>0</sup> within 8 minutes in the presence of 0.4 and 2.3 % (v/v) of water respectively, while the reduction in the absence of H<sub>2</sub>O was estimated to be 93.9 %. (See the ICP-OES results in Table S1)

At the early stage of the reaction, twin defects at the borders of combined tetrahedron of multiply twinned particles (MTPs) is the first sites for deposition of reduced silver atoms.<sup>14</sup> After

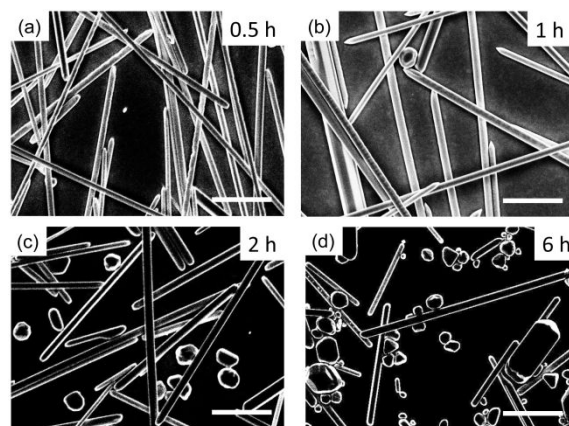


Fig. 2 SEM images of silver nanowires in the presence of 0.4 % (v/v) of H<sub>2</sub>O in EG kept at 160 °C for 30 min (a), 1 hour (b), 2 hours (c), and 6 hours (d), respectively, after the addition of AgNO<sub>3</sub> solution in the reaction. Scale bar is 1.5  $\mu\text{m}$ .

these borders are filled with silver atoms, the surface energy of facets of tetrahedron becomes larger than that of the first deposited sites. Then, covering of reduced silver atoms to MTPs starts, leading to longitudinal growth of AgNWs. Meanwhile, continuous etching of MTP with oxygen also occurs as long as the reaction proceeds under air. When water is added to the reaction mixture, the reduction rate of Ag<sup>+</sup> to Ag<sup>0</sup> is expected to be slower than the etching rate of MTP with oxygen, which could give a huge impact on the end morphology. In such a way, an appropriate amount of water most likely leads to the formation of sharp-end morphology. On the other hand, the excess amount of water over 0.8 % (v/v) leads to very low reduction rate, resulting in increase of shorter AgNWs (~ a few  $\mu\text{m}$ ) with various end morphologies and the entire bodies of AgNWs are etched (Fig. S3). The dependence of this water concentration is summarized in Table S2.

In order to understand the formulation mechanism of different end morphology in the presence of water, temporal evolution of the end shape was conducted. For this, SEM images of the product refluxed for 30 minutes, 1 hour, 2 hours and 6 hours after the addition of AgNO<sub>3</sub> solution were taken (Fig. 2). In this experiment, EG containing 0.4 % (v/v) water was used as solvent. At 30 minutes, the end morphologies of AgNWs are not uniform (Fig. 2a), while after 1 hour reflux most of AgNWs obtain sharp-end (Fig. 2b). When the reaction time is prolonged to more than 1 hour, production of AgNWs with rounded trapezoid end increases (Fig. 2c and 2d). According to the previous report,<sup>18</sup> dissolution of silver atoms at twinning defects and melting of MTPs by oxygen in air lead to the arcing of twin boundaries in MTPs and curving the surfaces of exposed {111} ends. In our reaction, the temperature was high enough to partially melt some of the MTPs and as a result, longer reaction time produces curved-surface MTPs that likely result in the formation of rounded trapezoid-end AgNWs. In addition to the production of AgNWs, many micrometre-sized nanoparticles are also found (Fig. 2c). At the latter reaction during the longer reaction time, the concentration of Ag<sup>+</sup> becomes lower, while oxidative etching rate

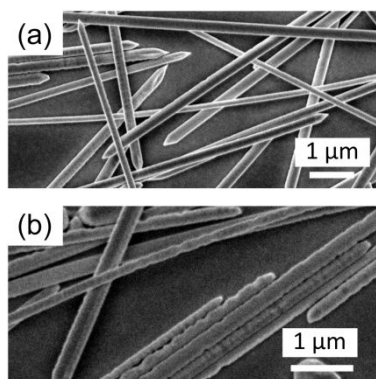


Fig. 3 SEM images of silver nanowires synthesized with different timing of water addition and inculcation temperature. (a) 100  $\mu\text{L}$  of water was added in the 14.7 mL reaction solution after the addition of  $\text{AgNO}_3$  and kept at 160  $^\circ\text{C}$  for 1 hour. (b) 100  $\mu\text{L}$  of water was added and kept at 160  $^\circ\text{C}$  for 30 minutes followed by another 100  $\mu\text{L}$  water injection and incubation at 160  $^\circ\text{C}$  for another 30 minutes.

is constant. Therefore, increasing the reaction time to 6 hours, less AgNWs are produced and alternatively various shapes of nanoparticles are produced in the solution (Fig. 2d) (See the summary in Table S3).

In the syntheses above, water was mixed with EG in advance. Now another question arises; which stage of the reaction does water play a role in formation of end morphology at? At the stage of the seed formation or growth process into nanowire? To address this question, only anhydrous EG was used to prepare all the precursor solutions and the timing of water injection was modified. Firstly, immediately after adding all  $\text{AgNO}_3$  solution, 100  $\mu\text{L}$  of Milli-Q was quickly injected into the reaction solution and the solution was kept stirring for further 1 hour at 160  $^\circ\text{C}$ . In this condition, similar to the second synthesis, almost all AgNWs have sharp ends (Fig. 3a). Secondly, when adding additional 100  $\mu\text{L}$  of water at 30 minutes reflux after the complete injection of  $\text{AgNO}_3$ , the entire body of AgNWs was etched and AgNWs ends were no longer sharp as shown in Fig. 3b. At the final stage of the reaction (after 30 minutes reflux), the concentration of  $\text{Ag}^+$  is much lower than the first stage of the reaction, while the addition of water at 30 min induces further deceleration of the reduction speed of  $\text{Ag}^+$ . Therefore, the oxidative etching of Ag happens much faster than the reduction, resulting in rough surface at the middle of nanowires and blunt end morphology. Note that adding water into  $\text{AgNO}_3$  EG solution produces sharp AgNWs with very low reproducibility and yield most likely because silver ions are partially reduced in the precursor solution before the injection. (Fig. S3)

As aforementioned, NLO response is sensitive to nanoscale structural change.<sup>27</sup> Since the end morphology of AgNWs is now controllable, we investigated dependence of end morphology on SHG properties of AgNWs (See the ESI). Since AgNWs serve as excellent plasmonic waveguide,<sup>7</sup> we investigated the possibility of remote excitation of SHG. In this experiment, fs laser was focused at one of AgNW sharp-ends (as indicated as 'in' in Fig. 4a) and out-coupling light at the distal end was monitored ('out' in Fig. 4a). As shown in Fig. 4a,

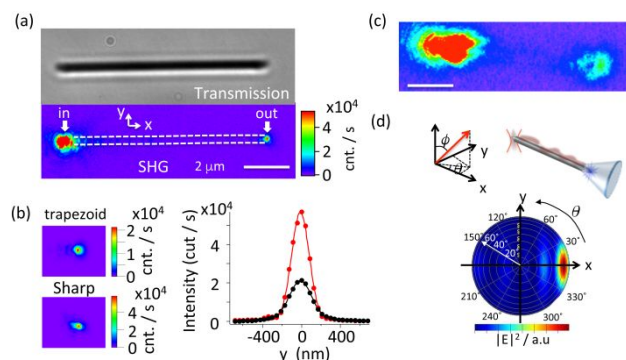


Fig. 4 (a) Remote excitation of SHG on a sharp-end AgNW. While 820 nm fs laser was focused at the left end of the nanowire, strong SHG signal was observed at the right end. The white dashed lines are eye guides to indicate the nanowire position. (b) The FWHM of SHG at out-coupling end of trapezoid (black) and sharp (red), respectively. (c) Defocused image of SHG. (d) Numerically calculated far-field projection of fan-out from the right end.

SHG was observed at the apex of nanowire's right end when the left end was irradiated by fs-laser. The spectra measurement proves that SHG was detected at ends but not at the middle of the NW (Fig. S4). Since 410 nm light hardly propagate along AgNWs (Fig. S5), it is most likely that propagating 820 nm SPPs was localized and induced SHG at the distal end.

The full-width half-maxima (FWHM) of the point spread function (PSF) of SHG along the transverse axes observed at the distal a sharp and trapezoid end are  $\sim 216$  and  $\sim 275$  nm, respectively (Fig. 4b). The FWHM is narrower and the SHG intensity is higher on sharp NWs, indicating LSPR is confined at smaller region and thus higher electromagnetic field enhancement at end of sharp NWs compared to that of trapezoid ones. Since SHG couples back to plasmon mode and re-emits from metal structure that disturbs PSF as recently demonstrated,<sup>3</sup> the actual size of the SHG spots at near-field are hardly estimated using far-field optical microscopy. Thus, localized surface plasmon resonance at a sharp AgNW end was numerically calculated using the finite-difference time-domain method. To mimic the experiment, 820 nm light was focused on one of AgNW end and electromagnetic (EM) field at the distal end was monitored (Fig. S6a). The simulation indicates tight localization of near-field EM field at the apex. Since the size of localized EM at end is estimated to be less than 10 nm (Fig. S6c-d), SHG should be also generated at nanoscale.

For application like near-field super-resolution microscopy, Poynting vector of emitting SHG from a nanowire end plays an important role. As shown in Fig. S7, the emitted SHG shows polarization parallel to the long axis of AgNW. This kind of polarization measurement, however, does not provide information regarding the direction of far-field scattering. Thus, the defocused image of SHG was taken, as it reflects the angular distribution of emission in PSF pattern.<sup>28, 29</sup> As shown in Fig. 4c, the defocus image shows two-lobe pattern with one lobe brighter than another. This asymmetric two-lobe defocused pattern suggests that the SHG radiates along the long axis in a direction toward outside of AgNW. To confirm this, a far-field projection of photon-radiation from an end of a

sharp AgNW was calculated from the FDTD simulation (Fig. 4d). Indeed, the far-field projection clearly shows the unidirectionality of Poynting vector from an end, where it propagates within  $\pm 15$  degree from the long axis. The SHG thus emit from an end of AgNW with a cone-angle of  $30^\circ$  as schematically illustrated in Fig. 4d, agreeing with a previous report<sup>30</sup>.

## Conclusions

In conclusion, synthesis of AgNWs with sharp ends has been developed through the slight modification of the well-known polyol synthesis. We found that water content in the solvent in the synthesis is the key to control end morphologies of AgNWs. The end shape can be controlled by varying the amount of water in the reaction solution and/or timing of water injection. Appropriate amount of water (0.2 ~ 0.4% (v/v)) together with proper reaction time (1 hour) provide pencil-like AgNWs with sharp end morphology in excellent yield over 90%. As an application, nonlinear optical effect, i.e. SHG, on the sharp nanowires was investigated. The SHG can be remotely generated through propagating plasmons on AgNWs. SHG emitted from a nanowire end shows uni-directional Poynting vector along the long axis of AgNWs. We suggest that the sharp-end AgNWs are suitable for nonlinear plasmonic applications, such as super resolution nonlinear optical microscopy and spectroscopy.

This work was supported by NAKATANI FOUNDATION to T.I. and H.U., JST PRESTO to KH, the Fund of Scientific Research–Flanders (FWO) and KU Leuven Internal Funds (C14/15/053). JSPS KAKENHI (17H03003, 18H01948, 18K19085) and JSPS Core-to-Core Program A. Advanced Research Networks are gratefully acknowledged. A part of this work was supported by the ‘Nanotechnology Platform’ in Hokkaido University. T.I. acknowledges the RIES International Exchange Program of ‘Dynamic Alliance for Open Innovation Bridging Human, Environment and Materials’ from MEXT.

## Conflicts of interest

There are no conflicts to declare.

## Author contribution

T.I. and H.U. developed the synthesis and conducted numerical simulation. S.T. and E.Y. conducted nonlinear experiments. T.I., G. L. and K. H. interpreted the mechanism of the synthesis. K.U., Y.T., B.L. and A.M. conducted and interpreted TEM measurements. Y.F. and H.U. designed the research.

## Notes and references

- M. W. Knight, N. K. Grady, R. Bardhan, F. Hao, P. Nordlander and N. J. Halas, *Nano Lett.*, 2007, **7**, 2346-2350.
- J. A. Hutchison, S. P. Centeno, H. Odaka, H. Fukumura, J. Hofkens and H. Uji-i, *Nano Lett.*, 2009, **9**, 995-1001.
- L. Su, G. Lu, B. Kenens, S. Rocha, E. Fron, H. Yuan, C. Chen, P. Van Dorpe, M. B. Roeffaers, H. Mizuno, J. Hofkens, J. A. Hutchison and H. Uji-i, *Nat. Commun.*, 2015, **6**, 6287.
- X. Ma, Y. Zhu, S. Kim, Q. Liu, P. Byrley, Y. Wei, J. Zhang, K. Jiang, S. Fan, R. Yan and M. Liu, *Nano Lett.*, 2016, **16**, 6896-6902.
- Y. Fujita, R. Chiba, G. Lu, N. N. Horimoto, S. Kajimoto, H. Fukumura and H. Uji-i, *Chem. Commun.*, 2014, **50**, 9839-9841.
- P. Walke, Y. Fujita, W. Peeters, S. Toyouchi, W. Frederickx, S. De Feyter and H. Uji-i, *Nanoscale*, 2018, **10**, 7556-7565.
- G. Lu, H. De Keersmaecker, L. Su, B. Kenens, S. Rocha, E. Fron, C. Chen, P. Van Dorpe, H. Mizuno, J. Hofkens, J. A. Hutchison and H. Uji-i, *Adv. Mater.*, 2014, **26**, 5124-5128.
- F. Fievet, J. P. Lagier, B. Blin, B. Beaudoin and M. Figlarz, *Solid State Ionics*, 1989, **32-33**, 198-205.
- G. Viau, F. Fievet-Vincent and F. Fievet, *Solid State Ionics*, 1996, **84**, 259-270.
- P. Toneguzzo, G. Viau, O. Acher, F. Fievet-Vincent and F. Fievet, *Adv. Mater.*, 1998, **10**, 1032-1035.
- F. Bonet, V. Delmas, S. Grugeon, R. H. Urbina, P. Y. Silvert and K. Tekaia-Elhsissen, *Nanostruct. Mater.*, 1999, **11**, 1277-1284.
- Y. G. Sun and Y. N. Xia, *Adv. Mater.*, 2002, **14**, 833-837.
- Y. G. Sun, B. Mayers, T. Herricks and Y. N. Xia, *Nano Lett.*, 2003, **3**, 955-960.
- B. Wiley, Y. G. Sun, B. Mayers and Y. N. Xia, *Chem. -Eur. J.*, 2005, **11**, 454-463.
- K. E. Korte, S. E. Skrabalak and Y. N. Xia, *J. Mater. Chem.*, 2008, **18**, 437-441.
- Y. G. Sun, Y. D. Yin, B. T. Mayers, T. Herricks and Y. N. Xia, *Chem. Mater.*, 2002, **14**, 4736-4745.
- S. Coskun, B. Aksoy and H. E. Unalan, *Cryst. Growth. Des.*, 2011, **11**, 4963-4969.
- S. H. Liu, B. M. Sun, J. G. Li and J. L. Chen, *Cryst. Eng. Comm.*, 2014, **16**, 244-251.
- A. Nekahi, S. P. H. Marashi and D. H. Fatmesari, *Mater. Chem. Phys.*, 2016, **184**, 130-137.
- A. Bouhelier, M. Beversluis, A. Hartschuh and L. Novotny, *Phys. Rev. Lett.*, 2003, **90**, 013903.
- C. Hubert, L. Billot, P. M. Adam, R. Bachelot, P. Royer, J. Grand, D. Gindre, K. D. Dorkenoo and A. Fort, *Appl. Phys. Lett.*, 2007, **90**, 181105.
- M. Danckwerts and L. Novotny, *Phys. Rev. Lett.*, 2007, **98**, 026104.
- Y. Zhang, F. Wen, Y. R. Zhen, P. Nordlander and N. J. Halas, *Proc. Natl. Acad. Sci. U. S. A.*, 2013, **110**, 9215-9219.
- M. Kauranen and A. V. Zayats, *Nat. Photonics*, 2012, **6**, 737-748.
- X. Xiong, C. L. Zou, X. F. Ren, A. P. Liu, Y. X. Ye, F. W. Sun and G. C. Guo, *Laser Photonics Rev.*, 2013, **7**, 901-919.
- Y. Fujita, P. Walke, S. De Feyter and H. Uji-i, *Jpn. J. Appl. Phys.*, 2016, **55**, 08NB03.
- J. Butet and O. J. F. Martin, *ACS Nano*, 2014, **8**, 4931-4939.
- M. Böhmer and J. Enderlein, *J. Opt. Soc. Am. B*, 2003, **20**, 554-559.
- H. Uji-i, S. M. Melnikov, A. Deres, G. Bergamini, F. De Schryver, A. Herrmann, K. Mullen, J. Enderlein and J. Hofkens, *Polymer*, 2006, **47**, 2511-2518.
- T. Shegai, V. D. Miljkovic, K. Bao, H. Xu, P. Nordlander, P. Johansson and M. Kall, *Nano Lett.*, 2011, **11**, 706-711.